Appl Phys B (2009) 95: 391–397
DOI 10.1007/s00340-009-3495-y

Applied Physics B
Lasers and Optics

Two-step holographic recording in photorefractive lithium niobate crystals using ultrashort laser pulses

C. Nölleke · J. Imbrock · C. Denz

Received: 19 December 2008 / Revised version: 16 February 2009 / Published online: 2 April 2009

Abstract We investigate non-volatile holographic data storage in photorefractive lithium niobate crystals. Infrared picosecond laser pulses are used to write holograms after sensitizing the crystal with blue light from a cw-laser. The dependence of the dynamic range and the photoconductivity on the pulse intensities and the recording wavelength is investigated in detail. The results can be explained by a two-center model if the mean intensity of the laser pulses is considered. We demonstrate that several fixed holograms can be multiplexed by employing the wavelength multiplexing technique.

PACS 42.65.Hw · 42.40.Ht · 42.70.Nq

1 Introduction

Photorefractive lithium niobate ($LiNbO_3$) crystals have been successfully utilized for the recording of volume phase holograms and they are one of the most promising materials for data storage applications due to their large storage densities [1]. Another advantage, its reversibility, is a disadvantage at the same time due to the "volatility" of the stored data. The most flexible approach for avoiding erasure of the holograms during read-out is the optical-fixing, or two-step recording technique [2], that allows non-volatile read-out of the stored holograms.

C. Nölleke · J. Imbrock · C. Denz (✉)
Institut für Angewandte Physik, Westfälische Wilhelms-Universität Münster, Corrensstr. 2/4, 48149 Münster, Germany
e-mail: denz@uni-muenster.de

The first holographic two-step recording experiments were performed with high intensity laser pulses in congruent $LiNbO_3$ crystals [2, 3]. Continuous-wave laser light was used to realize two-step recording in stoichiometric $LiNbO_3$ crystals as well [4–8].

A theoretical description of non-volatile recording is provided by the two-center model proposed by Jermann and Otten [9]. A detailed investigation of two-step recording using nanosecond pulses, along with a theoretical description, was reported in [10]. To the best of our knowledge, the process of optical fixing has not been investigated for picosecond pulses up to now. An understanding of the photorefractive effect in the ultrashort pulse regime, however, is important in order to speed up hologram writing processes and to exploit the potential for realizing applications that require short pulses as, e.g., optical switches (see, e.g., [11]). Especially, the question needs to be answered whether well-known models of the photorefractive response are still valid if ultrashort laser pulses are employed.

In this paper, we investigate two-step recording in near-stoichiometric $LiNbO_3$:Cu using picosecond pulses. Sensitizing is performed either with $\lambda = 400\,\mathrm{nm}$ laser pulses or $\lambda = 488\,\mathrm{nm}$ cw-laser light. Holograms are induced using pulsed laser light in the near-infrared spectral range. We determine the dynamic range and the photoconductivity for different light intensities and wavelengths.

2 Theoretical background

The recording of holograms in $LiNbO_3$:Cu is based on the photorefractive effect. This effect describes the build-up of an internal space-charge field E_{SC} induced by illumination with light and charge-transport processes inside the crystal. The charge-transport processes can be described with rate

equations in the so-called band-transport model [12, 13]. This model allows to calculate the dynamics of the photorefractive effect. Since the crystal is electro-optic, the electric field modulates the refractive index n. If the crystal is illuminated with an interference pattern, this pattern is mapped into a spatial variation of the refractive index. Therefore, holograms are stored typically as phase patterns. The relation between the electric field and the refractive index change Δn via the electro-optic effect is described by

$$\Delta n_{o,e} = -\frac{1}{2} n_{o,e}^3 r_{\text{eff}} E_{\text{SC}}, \tag{1}$$

where the indices o and e indicate ordinary and extraordinary polarization, respectively. Here, r_{eff} is the relevant element of the electro-optic tensor.

The principle of gated recording can be understood by means of a two-center charge transport model that was introduced by Jermann and Otten [9]. In this model, two photorefractive centers are taken into account (see Fig. 1). Copper dopants lead to Cu^+-centers that are "deep" levels (with respect to the conduction band), whereas the second center X^+ is more "shallow". Electrons can be excited from Cu^+ by light, forming Cu^{2+}. Electrons are excited either to the conduction band or to the shallow traps, resulting in the formation of the X^0 state.

The idea of two-step recording is the following: Light from the blue or green spectral range has sufficient photon energy to excite electrons from Cu^+ sites either into the conduction band or directly into the shallow centers, or from X^0 sites into the conduction band. Infrared photons, however, have insufficient energy for the excitation of electrons out of Cu^0 sites to the conduction band, but sufficient energy to excite electrons out of X^0 sites to the conduction band. By illuminating the crystal with visible light, shallow traps are filled, and the crystal will therefore be sensitized for subsequent holographic recording with infrared light out of X^0 centers.

Non-stoichiometric $LiNbO_3$ crystals always have a lithium deficit. Therefore, Nb-ions can be found on Li-sites and form an intrinsic defect Nb_{Li}^{5+}. On illumination, these centers can bound an electron and form a Nb_{Li}^{4+}-polaron (*small bound polaron*). From this center, electrons can be excited into the conduction band by light with infrared wavelength. Nb_{Li}^{5+} and Nb_{Li}^{4+} correspond to the more shallow centers previously denoted by X^+ and X^0, respectively.

Along with the presence of polarons, light-induced absorption occurs [14–17], which is an indication for a second photorefractive center and a necessary condition for the realization of two-step recording.

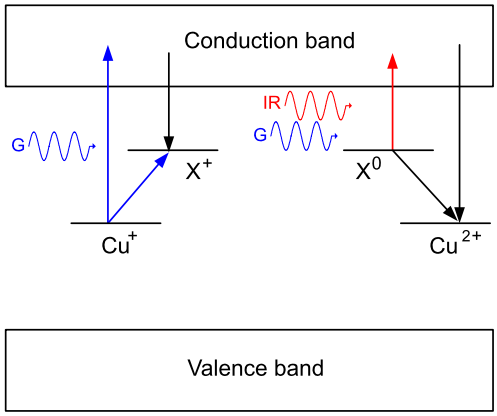

Fig. 1 The two-center model. $Cu^{+/2+}$ denote the deep traps, $X^{+/0}$ denote the shallow traps. G: Visible gating light; IR: Infrared recording light. The *arrows* indicate excitation and recombination of electrons

3 Experimental methods

The investigations presented in this paper are performed with a copper-doped near-stoichiometric $LiNbO_3$ crystal. The concentration of antisites is decreased with the help of a VTE (vapor transport equilibration) technique [19]. The result is an increased Li-content. The relative Li-content $c_{\text{Li}}/(c_{\text{Li}} + c_{\text{Nb}})$ is approximately 49.8% and is therefore close to a relative Li-content of 49.6%, where the holographic sensitivity shows its maximum value [8]. The photorefractive properties of these near-stoichiometric $LiNbO_3$:Cu crystals were investigated in detail with cw-laser light in a previous work [18]. The crystal has a thickness of $d = 1\,\text{mm}$. Its total copper concentration is $N_{\text{Cu}} = 156 \times 10^{23}\,\text{m}^{-3}$ whereas the concentration of Cu^+ is $N_{\text{Cu}}^- = 30 \times 10^{23}\,\text{m}^{-3}$.

Light-induced absorption changes that arise upon illumination of the crystals with visible light are measured in the following way: During pumping, the crystal is illuminated with either cw-light at 488 nm or picosecond pulse trains at 400 nm, and the transmitted intensity I_1^{t} of a probe beam (633 nm) behind the sample is detected with a photodiode. The coefficient for light-induced absorption is calculated by

$$\alpha_{\text{li}} = -\frac{1}{d} \ln\left(\frac{I_1^{\text{t}}}{I_0^{\text{t}}}\right), \tag{2}$$

where I_0^{t} is the transmitted intensity of the probe beam in the absence of the pump light, and d is the thickness of the sample.

The scheme of the holographic setup is shown in Fig. 2. Ordinary polarized pulses with a length of 1 ps and a repetition rate of $f_{\text{R}} = 1\,\text{kHz}$ from a tunable parametric amplifier overlap inside the crystal in space and time to generate elementary holographic gratings. The wavelength is tuned between 700 and 810 nm. The period length of the grating

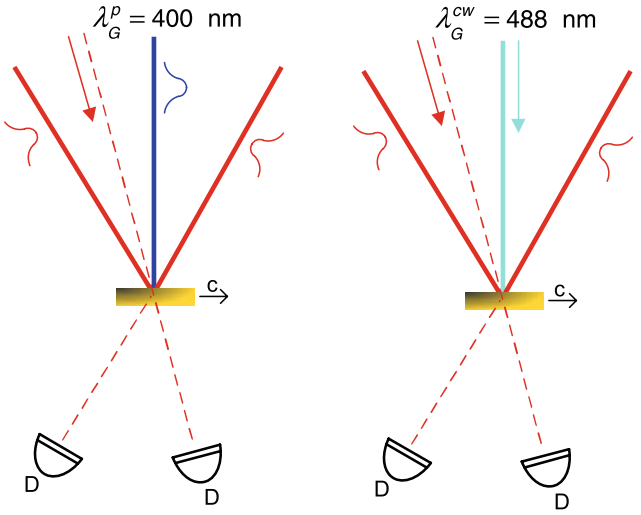

Fig. 2 Schematic diagram of the experimental setup for gating with pulsed light (*left*) or gating with cw-light (*right*). Intensities of diffracted and transmitted beams are measured with photodetectors (D)

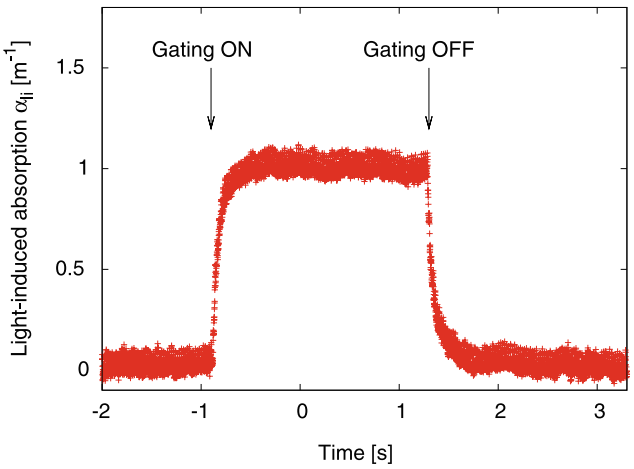

Fig. 3 Temporal course of the absorption change α_{li} induced by blue ($\lambda = 488$ nm) cw-laser light with an intensity of 5.3 kW/m^2. Here α_{li} increases when the gating light is turned on and decreases when it is turned off. From this measurement the lifetime of the polarons can be determined

depends on the wavelength and is approximately $\Lambda = 2$ µm. Light from a cw-laser (488 nm) illuminates the crystal homogeneously to perform the two-step process. Also 400-nm pulses having a length of 1 ps and a repetition rate of 1 kHz are used for sensitizing the crystal. In the latter case, we are able to tune the temporal delay of the gating pulses with respect to the infrared recording pulses. The intensities I_d and I_t of diffracted and transmitted extraordinarily polarized Bragg-matched He–Ne laser light are monitored using photodetectors. From these quantities the diffraction efficiency $\eta = I_d/(I_d + I_t)$ is determined. Using Kogelnik's formula [20],

$$\eta = \sin^2\left(\frac{\Delta n\,\pi\, d}{\lambda\cos\theta}\right), \tag{3}$$

we calculate the refractive index change Δn. Here θ is half of the angle between the recording beams inside the crystal.

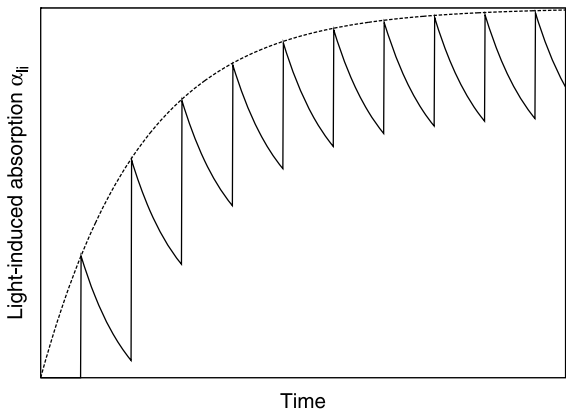

Fig. 4 Schematic diagram of the origin of the quasi-cw-behavior, when the lifetime τ_X of the polarons is much larger than the time T between successive pulses. The *solid line* shows the (magnified) temporal evolution of the light-induced absorption change after each pulse. On average the absorption increases exponentially with a time constant comparable with the lifetime of the polarons (*dashed curve*)

4 Light-induced absorption

Small light-induced absorption on the order of 1 m^{-1} is observed, that indicates the existence of small bound polarons. Monitoring α_{li} after turning off the gating light allows us to determine the lifetime of the polarons (see Fig. 3). We determined a value of approximately $\tau_X = 140$ ms. Therefore, the necessary condition for the two-step process is fulfilled. An important observation is, that the temporal development of the light-induced absorption is the same, if either cw-light or pulse trains are used to pump the system. A single shot does not produce any measurable light-induced absorption. This result can be explained as a *quasi-cw-behavior* for pulse trains. As an illustration, Fig. 4 shows the build-up of the light-induced absorption upon pulse illumination. Each pulse leads to an instantaneous generation of polarons that corresponds to a delta-like increase of the light-induced absorption. The electrons from shallow traps decay into deep traps, so that the absorption decreases exponentially. Since the lifetime τ_X of the polarons is much greater than the time between two adjacent pulses $T = 1/f_R$, only a small fraction of about 1% of polarons has been decayed when the next pulse arrives. After approximately 100 ms a saturation value is reached, the *quasi-steady-state*, where the density of filled shallow traps is almost constant. Using a cw-laser leads to the same development of the light-induced absorption, and the saturation values for cw- and pulsed-light with the same mean intensities are nearly identical. This behav-

ior can be explained in terms of the two-center model (see Fig. 1). The light-induced absorption α_{li} is proportional to the concentration of filled shallow traps N_{X}^{-}:

$$\alpha_{\mathrm{li}} \propto N_{\mathrm{X}}^{-}. \tag{4}$$

To calculate the concentration N_{X}^{-} under illumination one has to solve the corresponding rate equation [9]:

$$\frac{\partial N_{\mathrm{X}}^{-}}{\partial t} = -\left[\beta_{\mathrm{X}} + s_{\mathrm{X}} I_{\mathrm{G}} + \gamma_{\mathrm{XCu}}(N_{\mathrm{Cu}} - N_{\mathrm{Cu}}^{-})\right] N_{\mathrm{X}}^{-} + (\gamma_{\mathrm{X}} N + s_{\mathrm{CuX}} I_{\mathrm{G}} N_{\mathrm{Cu}}^{-})(N_{\mathrm{X}} - N_{\mathrm{X}}^{-}), \tag{5}$$

with the gating intensity I_{G}, copper concentration N_{Cu}, concentration of Cu^{+} N_{Cu}^{-}, and the concentration N_{X} of shallow traps. Here β_{X} denotes the coefficient for thermal excitation of electrons from X^{0} centers to the conduction band, γ_{XCu} is the coefficient for recombination of electrons from filled shallow traps to Cu^{2+}, s_{CuX} is the absorption cross section for the excitation of an electron from Cu^{+} directly to an empty shallow trap, and s_{X} denotes the cross section of shallow traps for the excitation of an electron to the conduction band. If one assumes that the shallow traps are mainly populated with electrons directly out of deep centers and that during the illumination the concentration N_{Cu}^{-} of Cu^{+} changes only slightly, like in iron-doped $\mathrm{LiNbO_3}$ [9], (5) yields the concentration of filled shallow traps:

$$N_{\mathrm{X}}^{-} = s_{\mathrm{CuX}} I_{\mathrm{G}} N_{\mathrm{Cu}}^{-} N_{\mathrm{X}} \tau \left[1 - \exp\left(-t/\tau\right)\right], \tag{6}$$

with the inverse time constant

$$1/\tau = \beta_{\mathrm{X}} + \gamma_{\mathrm{XCu}}(N_{\mathrm{Cu}} - N_{\mathrm{Cu}}^{-}) + s_{\mathrm{X}} I_{\mathrm{G}}(N_{\mathrm{Cu}}^{-} + N_{\mathrm{X}}). \tag{7}$$

Then, the relaxation of the filled shallow traps in the dark should follow an exponential decay with the time constant τ_{X}:

$$1/\tau_{\mathrm{X}} = 1/\left(\beta_{\mathrm{X}} + \gamma_{\mathrm{XCu}}(N_{\mathrm{Cu}} - N_{\mathrm{Cu}}^{-})\right). \tag{8}$$

If the pulse length t_{P} is shorter than the lifetime of the polarons τ_{X}, the polaron concentration increases linearly with increasing donor concentration N_{Cu}^{-} and pulse length:

$$N_{\mathrm{X}}^{-} = s_{\mathrm{CuX}} I_{\mathrm{G}} N_{\mathrm{Cu}}^{-} N_{\mathrm{X}} t_{\mathrm{P}}. \tag{9}$$

This expression is valid for the illumination with single nanosecond laser pulses [9, 10, 21]. In our case, the polaron lifetime of 140 ms is much larger than the pulse length of 1 ps but one single picosecond pulse does not lead to any measurable absorption change since the energy $E \propto I_{\mathrm{G}} t_{\mathrm{P}}$ of one pulse is too small to increase the polaron concentration N_{X}^{-} significantly. If the reciprocal repetition rate is much smaller than τ_{X}, the steady state value of the polaron concentration ($t \to \infty$ in (6)) depends linearly on the lifetime of the polarons τ_{X}:

$$N_{\mathrm{X}}^{-} = s_{\mathrm{CuX}} I_{\mathrm{G}} N_{\mathrm{Cu}}^{-} N_{\mathrm{X}} \tau_{\mathrm{X}} \tag{10}$$

$$= \frac{s_{\mathrm{CuX}} I_{\mathrm{G}} N_{\mathrm{Cu}}^{-} N_{\mathrm{X}}}{\beta_{\mathrm{X}} + \gamma_{\mathrm{XCu}}(N_{\mathrm{Cu}} - N_{\mathrm{Cu}}^{-}) + s_{\mathrm{X}} I_{\mathrm{G}}(N_{\mathrm{Cu}}^{-} + N_{\mathrm{X}})}. \tag{11}$$

This expression should also be valid for illumination with cw-laser light. In our case, the reciprocal repetition rate of 1 ms is much smaller than the polaron lifetime of about 140 ms, i.e., we can assume a quasi-cw-behavior.

The lifetime of polarons in the near-stoichiometric $\mathrm{LiNbO_3}$:Cu crystal is much larger than the polaron lifetime in doped and undoped congruently melting $\mathrm{LiNbO_3}$ crystals, where the lifetime is normally in the microsecond range [21, 22]. The reason for the increased lifetime is the concentration of Cu^{2+} and $\mathrm{Nb_{Li}}$ defects. The polaron lifetime likely depends on the distance between filled shallow traps and Cu^{2+} like in iron-doped $\mathrm{LiNbO_3}$ and $\mathrm{LiTaO_3}$ crystals [21, 23]. During the VTE treatment Li ions diffuse into the crystal, and therefore the concentration of $\mathrm{Nb_{Li}}$ defects decreases. Simultaneously, the distance between $\mathrm{Nb_{Li}}$ defects and Cu^{2+} ions increases, resulting in an increased polaron lifetime.

5 Holographic recording

$\mathrm{LiNbO_3}$:Cu is insensitive for holographic recording with infrared light. Infrared recording becomes possible if the crystal is illuminated homogeneously with visible light (cw-light at 488 nm or pulse trains at 400 nm, respectively) at the same time. An at first glance surprising result is, that the variation of the temporal delay between gating and write pulses has no influence on the write cycles, if pulse trains are used for sensitizing. This observation fits to the previous explained quasi-cw behavior for the light-induced absorption. Figure 4 shows the origin of the quasi-steady-state, where the density of filled shallow traps reaches a saturation value. Obviously, the magnitude of this density does not depend on a temporal delay between gating and recording pulses, and consequently such a delay does not have any influence on the experimental results. Since the magnitude of the light-induced absorption and consequently the density of polarons are the same for cw- and pulsed-light, two-step recording works with pulsed- and cw-light, provided that the mean intensity is of the same order of magnitude.

Figure 5 shows a typical write–read–erase cycle. In the first part, the infrared light and the visible light impinge on the crystal at the same time and the refractive index changes increase. The second part shows the non-destructive readout process, where only one of the infrared beams is used.

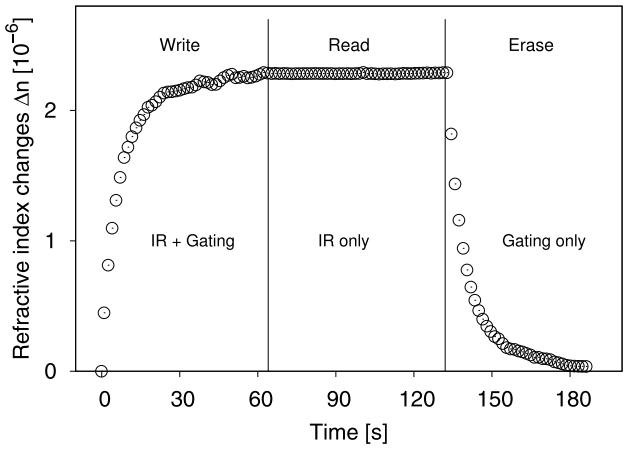

Fig. 5 Typical write–read–erase cycle. The crystal was sensitized with cw-light at 488 nm and $I_G = 5.3$ kW/m^2. Recording was performed with pulsed light at 800 nm and $I_{IR} = 3.2$ kW/m^2

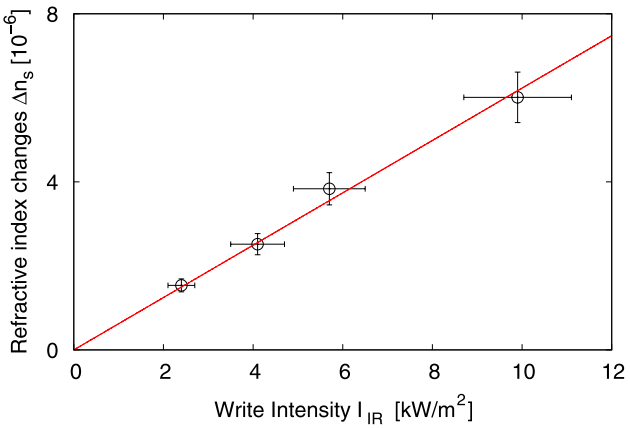

Fig. 6 Saturation values Δn_s of refractive index changes as a function of the intensity I_{IR} of the writing light. The gating intensity was fixed at $I_G = 5.3$ kW/m^2. The writing wavelength was $\lambda = 810$ nm. The *line* is a linear fit to the measured values

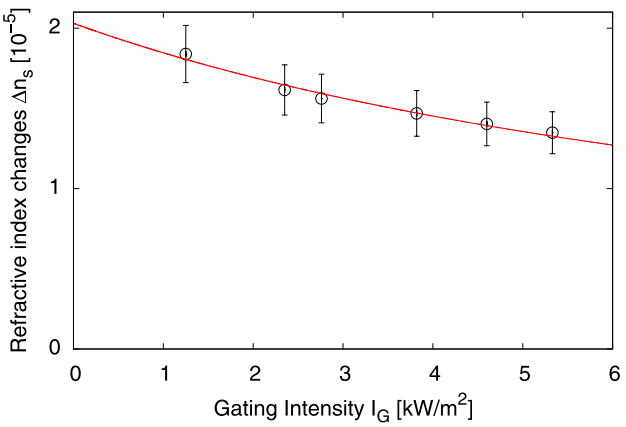

Fig. 7 Saturation values Δn_s of refractive index changes as a function of the gating intensity I_G. The intensity of the writing light was fixed at $I_{IR} = 20.8$ kW/m^2. The writing wavelength was $\lambda = 750$ nm. The *curve* is a fit according to (15)

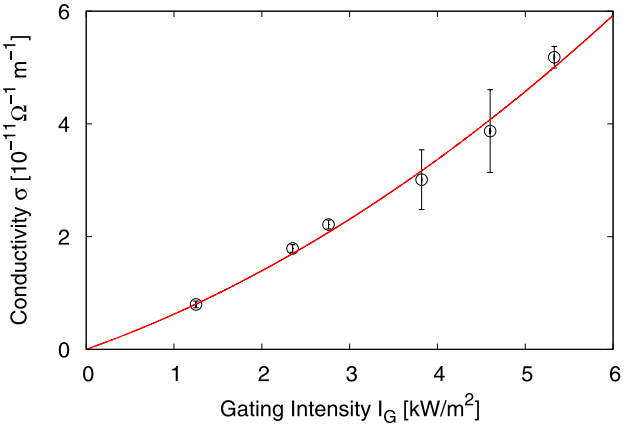

Fig. 8 Photoconductivity σ_{ph} as a function of the gating intensity I_G. The intensity of the writing light was fixed at $I_{IR} = 20.8$ kW/m^2. The writing wavelength was $\lambda = 750$ nm. The *curve* is a fit according to (16)

Erasing of the hologram is performed by illuminating the crystal homogeneously with sensitizing light. The temporal behavior of the refractive index changes is well-described by mono-exponential fits. From these measurements, the saturation refractive index change (*dynamic range*) Δn_s and the time constants τ, and therefore the photoconductivity σ_{ph}, are determined [12, 13]. For a fixed wavelength, Δn_s depends always linear on the write intensity I_{IR} and no saturation is observed, whereas Δn_s depends only weakly on the gating intensity I_G (Figs. 6 and 7). The photoconductivity is a sublinear function of the gating intensity, whereas the dependence on the write intensity is weak (Figs. 8 and 9).

Nonvolatile holographic recording can be explained within the two-center model. The question arises, whether the well-known models for cw-illumination are valid in the case of ultrashort laser pulses. Okamura showed that the one-center model remains valid for the case of mode-locked pulse trains, if the mean intensity

$$\langle I \rangle = \langle I(t) \rangle = \frac{1}{T} \int_0^T I(t)\,\mathrm{d}t \tag{12}$$

of the pulses is used in the rate-equations [24]. Here $f_R = 1/T$ is the repetition rate of the laser. In this model, the *very short pulse illumination* (*VSPI*) *approximation* is used, where the charge carriers migrate, diffuse, and drift in the dark, assuming that the carrier-density distribution is given as an initial condition after the pulse arrives [25]. We expand this result to the two-center model. If we take the analytic analysis of the two-center model for nanosecond pulses [26]

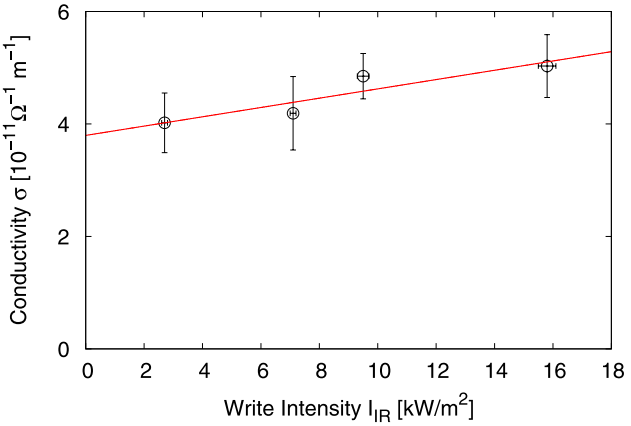

Fig. 9 Photoconductivity σ_{ph} as a function of the intensity I_{IR} of the writing light. The gating intensity was fixed at $I_{\text{G}} = 5.3\,\text{kW/m}^2$. The writing wavelength was $\lambda = 800$ nm. The *line* is a linear fit

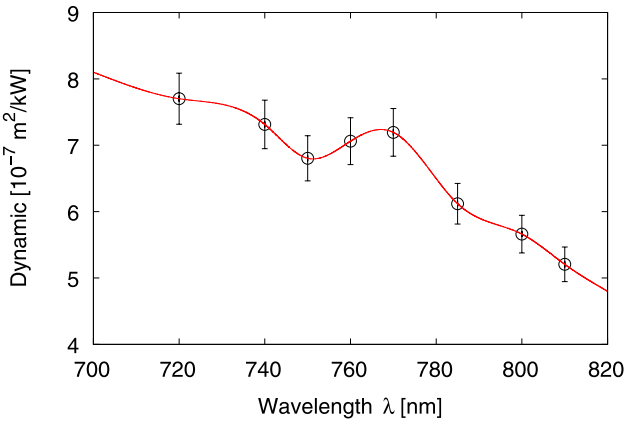

Fig. 10 Wavelength dependence of the *dynamic* $\mathcal{D}$ as defined in (17). The *curve* is a spline fit and serves as a guide to the eye

and take into account the mean intensities, we end up at

$$E_{\text{SC}} \approx m \frac{\kappa_{\text{X}}^{\text{IR}} \langle N_{\text{X}}^{-} \rangle \langle I_{\text{IR}} \rangle}{e\mu \langle N \rangle} \tag{13}$$

for the saturation space-charge field and at

$$\sigma_{\text{ph}} = e\mu \langle N \rangle = \frac{\epsilon \epsilon_0}{\tau} \tag{14}$$

for the photoconductivity. The brackets $\langle \cdot \rangle$ denote the mean values. Here $\kappa_{\text{X}}^{\text{IR}}$ is the photovoltaic coefficient, μ denotes the electron mobility, and ϵ_0 is the permittivity of free-space. For $LiNbO_3$ the dielectric coefficient is $\epsilon = 28.7$ [27]. For small sensitizing intensities the polaron concentration N_{X}^{-} (11) as well as the density of electrons N increase linearly with increasing sensitizing intensity. Therefore, when the sensitizing intensity decreases, the space-charge field converges to a constant value. Obviously, a space-charge field cannot build up without any sensitizing light. On the other hand, with increasing sensitizing intensity the polaron concentration N_{X}^{-} (11) tends to saturate, while the photoconductivity still increases. Hence, the space-charge field tends to zero with increasing sensitizing intensity. Considering (1), (11), and (13), one gets the following result for the dependence of the refractive index changes on the light intensities:

$$\Delta n_{\text{S}} \propto \frac{\langle I_{\text{IR}} \rangle}{\text{const} + \langle I_{\text{G}} \rangle}, \tag{15}$$

which is in good agreement with the experimental results (Figs. 6 and 7). As discussed in [26], (14) implies the relation

$$\sigma_{\text{ph}} = \text{a} \langle I_{\text{G}} \rangle + \text{b} \langle I_{\text{G}}^2 \rangle, \tag{16}$$

and is confirmed by our experimental results (Fig. 8). These facts suggest that the VSPI approximation is also valid for the picosecond pulses used in the case of two photorefractive centers.

6 Spectral dependence of the dynamic range

To investigate the spectral dependence of the dynamic range, we define a new quantity, the *dynamic* $\mathcal{D}$

$$\mathcal{D} = \frac{\Delta n_{\text{s}}}{m I_{\text{IR}}}, \tag{17}$$

where m is the modulation of the holographic grating. The *dynamic* serves as a figure of merit for the dynamic range for a given writing intensity and a given wavelength of the writing light. It is measured for different wavelengths between 700 and 810 nm. Figure 10 shows the result. A decrease for infrared light and an increase for visible light can be observed. At approximately 760 nm we found a maximum that may be related to the maximum of the absorption cross-section for polarons [8]. The decrease of the *dynamic* $\mathcal{D}$ is also expected from the polaron spectrum. The increase for visible light is not fully understood. It is reasonable, that there are two main processes which lead to this observation. First, $LiNbO_3$:Cu becomes more sensitive for visible light, due to direct excitations from deep traps into the conduction band, that are more probable for smaller wavelengths. Second, the use of ultrashort laser pulses with high peak intensity may result to two-photon absorption processes out of the deep traps into the conduction band, which is also more probable for smaller wavelengths.

7 Wavelength multiplexing

The two-step recording process is ideally-suited to realize multiplexing in volume holographic storage applications due to its nonvolatile features. Here, we employ wavelength multiplexing [28] by simply changing the wavelength of the parametric amplifier and using the sequential recording scheme [29] to record multiple optical fixed holograms

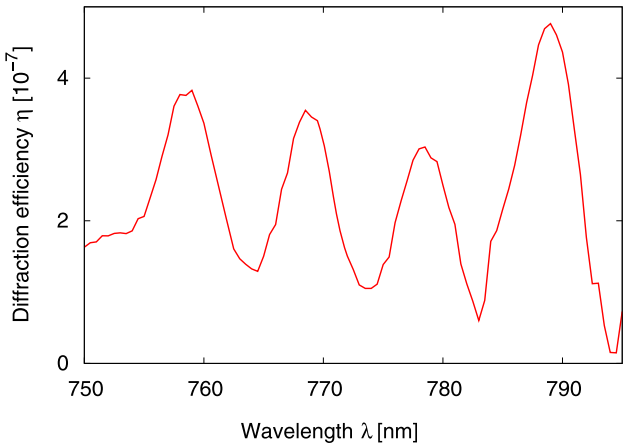

Fig. 11 Superposition of four holograms in the same volume element inside the crystal. Recording was performed using the two-step process

at the same place inside the photorefractive crystal sample. The holograms are read-out independently by choosing the wavelength used for recording.

Figure 11 shows a first result of the diffraction efficiency of four multiplexed holograms in the near-infrared spectral region. We could show that the same results are obtained for incremental recording [30]. The spectral distance between adjacent holograms is chosen to be 10 nm to avoid considerable cross-talk. The slightly different diffraction efficiencies are due to an imperfect recording schedule. The Bragg selectivity is quiet broad for holograms that are multiplexed with picosecond laser pulses because the holograms are written and read-out with pulsed laser light of a broad spectrum in comparison to cw-laser experiments. The bandwidth (FWHM) of one pulse with a duration of 1 ps and a wavelength of 770 nm is approximately 2 nm. Therefore, the Bragg selectivity (Fig. 11) can be calculated as a convolution of the spectrum of the recorded grating and the spectrum of the read-out light. This leads to a spectral width of the diffraction efficiency of about 3 nm of the multiplexed holograms that fits well to the experimental value of 4 nm.

8 Conclusions

We demonstrated the possibility for gated recording in the ultrashort regime. Sensitizing of the crystal is possible with either pulsed or cw-light. This fact can be explained with the discussed quasi-cw-behavior for pulse trains. For a theoretical description we used the VSPI approximation and the well-known two-center model for nanosecond pulses. In substance, this model remains valid, if all variable quantities are replaced by their mean values.

Tuning the recording wavelength, we determined the spectral dependence of the dynamic. The maximum at about 760 nm corresponds to the maximum of the absorption cross-section of polarons.

We demonstrated that the wavelength multiplexing technique can be combined with the principle of gated recording. This result may be important for data storage application, where efficient, high-density, non-volatile storage media are desirable.

Acknowledgements The authors like to thank Prof. Dr. M. Imlau of the University of Osnabrück for providing the $LiNbO_3$ crystals.

References

1. H. Coufal, D. Psaltis, G. Sincerbox, *Holographic Data Storage* (Springer, New York, 2000)
2. D. von der Linde, A.M. Glass, K.F. Rodgers, Appl. Phys. Lett. **25**, 155 (1974)
3. K. Buse, F. Jermann, E. Krätzig, Ferroelectrics **141**, 197 (1993)
4. Y.S. Bai, R.R. Neurgaonkar, R. Kachru, Opt. Lett. **21**, 567 (1996)
5. Y.S. Bai, R. Kachru, Phys. Rev. Lett. **78**, 2944 (1997)
6. H. Guenther, G. Wittmann, R.M. Macfarlane, R.R. Neurgaonkar, Opt. Lett. **22**, 1305 (1997)
7. H. Guenther, R. Macfarlane, Y. Furukawa, K. Kitamura, R.R. Neurgaonkar, Appl. Opt. **37**(32), 7611 (1998)
8. L. Hesselink, S.S. Orlov, A. Liu, A. Akella, D. Lande, R.R. Neurgaonkar, Science **282**, 1089 (1998)
9. F. Jermann, J. Otten, J. Opt. Soc. Am. B **10**, 2085 (1993)
10. J. Imbrock, S. Wevering, K. Buse, E. Krätzig, J. Opt. Soc. Am. B **26**, 1392 (1999)
11. L. Aronson, L. Hesselink, Opt. Lett. **15**(1), 20 (1990)
12. N.V. Kukhtarev, V. Markov, S. Odulov, M. Soskin, V. Vinetskii, Ferroelectrics **22**, 949 (1979)
13. N.V. Kukhtarev, V. Markov, S. Odulov, M. Soskin, V. Vinetskii, Ferroelectrics **22**, 961 (1979)
14. O. Schirmer, D. von der Linde, Appl. Phys. Lett. **33**, 35 (1978)
15. F. Jermann, M. Simon, E. Krätzig, J. Opt. Soc. Am. B **12**, 2066 (1995)
16. G. Ming, S. Kapphan, R. Pankrath, X. Feng, Y. Tang, V. Vikhnin, J. Phys. Chem. Solids **61**, 1775 (2000)
17. P. Herth, T. Granzow, D. Schaniel, T. Woike, M. Imlau, E. Krätzig, J. Opt. Soc. Am. B **95**, 067404 (2005)
18. J. Imbrock, A. Wirp, D. Kip, E. Krätzig, D. Berben, J. Opt. Soc. Am. B **19**, 1822 (2002)
19. D.H. Jundt, M.M. Fejer, R.L. Byer, IEEE J. Quantum Electron. **26**, 135 (1990)
20. H. Kogelnik, Bell. Syst. Tech. J. **48**, 2909 (1969)
21. D. Berben, K. Buse, S. Wevering, P. Herth, M. Imlau, T. Woike, J. Appl. Phys. **87**, 1034 (2000)
22. O. Beyer, D. Maxein, T. Woike, K. Buse, Appl. Phys. B **83**, 527 (2006)
23. S. Wevering, J. Imbrock, E. Krätzig, J. Opt. Soc. Am. B **18**, 472 (2001)
24. H. Okamura, J. Opt. Soc. Am. B **18**, 960 (2001)
25. G.C. Valley, IEEE J. Quantum Electron. **QE-19**, 1637 (1983)
26. A. Adibi, K. Buse, D. Psaltis, Phys. Rev. A **63**, 023813 (2001)
27. R.T. Smith, F.S. Welsh, J. Appl. Phys. **42**, 2219 (1971)
28. S. Yin, H. Zhou, M. Wen, Z. Yang, J. Zhang, F.T.S. Yu, Opt. Commun. **101**, 317 (1993)
29. A. Strasser, E. Maniloff, K. Johnson, S. Goggin, Opt. Lett. **14**, 6 (1989)
30. Y. Taketomi, J. Ford, H. Sasaki, J. Ma, Y. Fainman, S. Lee, Opt. Lett. **16**, 1774 (1991)